toward the walls. This interaction mechanism also occurs (Fig. 2) when the interparticle distance exceeds their characteristic size by 5 times and more. This fact, on one hand, justifies the assumption made above concerning flow in the "single" particle regime, and, on the other hand, implies that for variations in the flow structure in the SW zone the deviation between particles discarded from the body flow might be small.

The transmission problem of an SW front by particles moving toward the supersonic flow was first generated in experimental studies of flow around bodies filled by a hypersonic flow [4, 5]. It has been established that as a result of the interaction of the shock layer with particles rebounding from the flow surface an SW perturbation is generated.

The perturbations were manifested in the form of conical abrupt changes, traveling above the flow. The experimental technique used, however, did not allow for a complete explanation of the internal flow structure generated in the case, which, in turn, made it difficult to explain the effects observed. Thus, it was noted in [5] that a particle is not found in all perturbed sudden changes, and that in several cases, when there are no particles in the apex of the conical discontinuity, the apex is not closed. It was also established in [5] that the half-angles of conical perturbations with particles in the apex are smaller than the half-angles of the discontinuity opening, but there are no particles in the apex. This is also verified by the calculations described above: the SW front formed at the vortices are steeper than the conical discontinuity generated at the particle (see Figs. 1 and 2).

LITERATURE CITED

1. V. I. Blagosklonov, V. M. Kuznetsov, et al., "The interaction of hypersonic non-single-phase flows," Prikl. Mekh. Tekh. Fiz., No. 5 (1979).
2. N. P. Gridnev, "A difference scheme of third order accuracy for the calculation of complex gas-dynamic and magnetohydrodynamic flows," in: Problems of Magnetic Gas Dynamics [in Russian], ITPM Siber. Otdel. Akad. Nauk SSSR, Novosibirsk (1979).
3. G. N. Abramovich, Applied Gas Dynamics [in Russian], Nauka, Moscow (1969).
4. L. E. Dunbar, J. F. Courtney, and L. D. McMillen, "Heating augmentation in erosive hypersonic environments," AIAA J., 13, No. 7 (1975).
5. D. T. Hove and A. A. Smith, "Holographic analysis of particle-induced hypersonic bow-shock distortions," AIAA J., 13, No. 7 (1975).

MAGNETOIMPULSIVE GENERATION OF A CUMULATIVE COMPRESSION WAVE

S. G. Alikhanov and V. P. Bakhmin

UDC 539.893+62-987/-988

The importance of obtaining high pressures is well known. Scientific investigators have achieved particularly significant results in this direction through dynamic methods based on the use of powerful shock waves generated by one means or another [1-4]. However, even if we ignore the specific difficulties inherent in these methods, they may not be usable because in many cases they require a smooth (non-shock) increase in pressure. The problem of obtaining such pressures is solved relatively easily by the use of magnetic fields. For example, [5] described experiments involving the isentropic compression of organic glass to 400 GPa by a magnetic field directed along the axis of a copper tube containing the test specimen. The magnetic field was intensified to a magnitude corresponding to a pressure of 400 GPa (~10 MG) by compressing it with a steel tube accelerated by products from the detonation of an explosive and positioned coaxially with the copper tube. A similar geometry was used in [6], which reported on the phase transformation of quartz to the super-dense state at a pressure of 125 MPa. This state had not been observed in tests with shock waves. The use of explosives in experiments of the type just described, however, may limit the range of application of this method of developing high pressures. Attention is thus being given to another possible use of impulsive magnetic fields: to compress the test substance with a shell

Moscow. Translated from Zhurnal Prikladnoi Mekhaniki i Tekhnicheskoi Fiziki, No. 2, pp. 118-123, March-April, 1987. Original article submitted January 20, 1986.

0021-8944/87/2802-0272$12.50

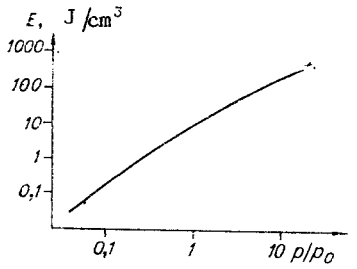

Fig. 1

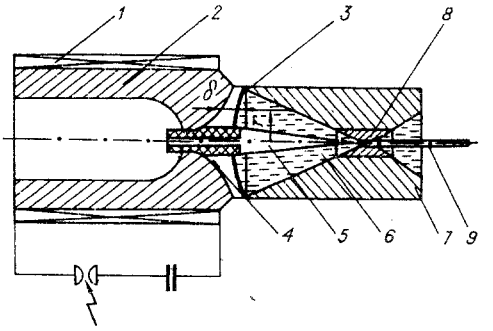

Fig. 2

accelerated by the pressure of the magnetic field associated with an electric current passed through the shell upon the discharge of a capacitor. The authors of [7], employing a cylindrical geometry, succeeded in compressing gaseous helium to a pressure of 8 GPa. In [8], a similar geometry was used to obtain even higher pressures: gaseous hydrogen was compressed to about 20 GPa. However, this method of producing high pressures also has shortcomings: even if the specimen is initially solid, it, the shell, and certain parts of the working chamber undergo failure, and it is possible only to record the fact that a high pressure was obtained in the specimen — not the result of this pressure. In connection with this, the most suitable systems for experiments may prove to be those with a low level of energy in the "propellant" element and which concentrate the energy density in the transmitting medium.

The goal of the present study is to explain the features, potential, and limitations of magnetoimpulsive generation of a cumulative compression wave. We will use the specific example of wave excitation in a conical cavity filled with water.

If we represent the pressure dependence of energy density for water (Fig. 1), having used [9] $p = p_0[(\rho/\rho_0)^7 - 1]$ ($p_0 = 0.3$ GPa, ρ_0 and ρ are the initial and running density of the water), it becomes apparent that an increase in energy density by a factor of 100 will increase p by more than one order of magnitude with an initial pressure of, say, 30 MPa ($p/p_0 = 0.1$). Also, although the relationship between energy density and pressure is nonlinear, the increase in the initial pressure in the compression pulse may be substantial even with a moderate concentration of energy. Such a concentration would not be hard to achieve, given the appropriate geometry.

We used the unit depicted in Fig. 2 to generate and intensity a compression wave in water by means of an impulsive magnetic field. A magnetic flux passed through 2 lengthwise slits (not shown) in a "magnetic hammer" 2 located inside a single-layer coil 1 when a capacitor battery (18 banks of the IK-50-3 type) discharged on the coil. The coil had an inside diameter of 30 cm and a length of 70 cm and consisted of 14 sections of 10 turns each. The sections were connected in parallel. Since the piston (duralumin) was thicker than the skin layer, the magnetic flux was concentrated in the gap formed by the end of the hammer and the piston. If the shape of the end surface of the hammer was such that $r\delta = \text{const}$ (δ is the size of the gap — with allowance for the skin layer — between the hammer face and the piston at the distance r from the axis of the system), then the magnetic field in the gap would be constant. In this case, with the passage of current through the coil the piston was subjected to a pressure equal to $\mu_0 H^2/2$ and distributed uniformly over the entire surface. Here, μ_0 is the magnetic permeability of a vacuum and H is the magnetic field in the gap. This field was measured with a magnetic probe 4. In the present simplified examination, we ignore the effect of the curvature of the magnetic lines of force. Since a field on the order of 200 kG (this corresponds to a pressure of 160 MPa on the diaphragm) can be withstood by ordinary structural materials, it is fairly simple to create a system with a pressure of 100-200 MPa near the piston. The condition $r\delta = \text{const}$ is not satisfied in the central region, so it turned out to be necessary to introduce an internal cone 5. This cone had a base with a diameter of 5 cm and a length of 45 cm. Introduction of the cone reduced the solid angle for the cumulative wave by 6%.

The piston has the form of a spherical segment of 50 cm radius, with a base 20 cm in diameter and a central hole of 5 cm (for the cone). The piston is displaced under the influence of the magnetic field, and a pressure pulse or compression wave with a spherical front is generated in the water 6 which fills the concentrator 7. The concentrator has a conical

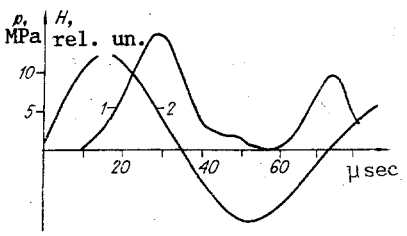

Fig. 3

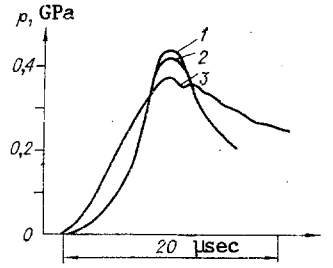

Fig. 4

cavity and a replaceable insert 8. The wave front is bounded by the conical surfaces of the concentrator and cone. The amplitude and length of the wave are ultimately determined by the parameters of the electrical circuit and the speed of sound in the water. In principle, they may vary broadly. Since they are always the same with fixed parameters for the current passing through the coil, the pressure in the wave – at least near the piston – will always be the same, assuming that the piston is returned to its original position after each test. Return of the piston can easily be incorporated into the design of the testing equipment.

The amplitude of the compression wave increases as it recedes from the piston, since the process of accumulation increases the energy density in the wave. This highest pressure is reached at the outlet of the concentrator, near the geometric center of accumulation. The piezoelectric sensor 9 is located here.

The amplitude of the wave at any distance from the accumulation center R_1 can be easily evaluated if we know the amplitude near the piston, i.e., at the distance R_0 from the center. For this, it is sufficient to equate the energy of the pressure pulse at the distances R_0 and R_1. This presumes that dissipation is slight. Without allowance for dispersion, after several transformations we obtain the relation

$$\frac{E_1}{E_0} \simeq 2\frac{R_0^3-(R_0-\lambda)^3}{R_1^3-(R_1-\lambda)^3},$$

where E_0 and E_1 are the energy densities in the pulse at the distances R_0 and R_1; λ is the length of the pressure pulse. In this relation, we considered the fact that the energy density of the wave doubles when it stops, since the kinetic energy of the pressure pulse is roughly equal to the compressive energy. In the unit being used here, R_0 = 50 cm, $\lambda \simeq$ 3 cm, and the wave stops at the distances R_1 = 3 cm and R_2 = 1.5 cm. These values were specified on the basis of the size of the hole for the pressure sensor in the insert 8 (see Fig. 2). The situation just described corresponds to an accumulation of energy density by factors of roughly 300 and 500 and an increase in pressure by factors of 18 and 30, respectively, with a pressure pulse having an initial amplitude of 20 MPa, in accordance with Fig. 1.

The initial pressure in the pressure pulse was measured near the piston by three piezoelectric sensors positioned at different distances from the axis of the system. The sensitive element of each sensor was a disk of piezoceramic TsTS-19 with a diameter of 5 mm (or 2 mm) and a thickness of 1 mm. Using lead washers 0.5 mm thick, we mechanically secured the disk between receiving (length 0.5 cm) and regulating (length 30 cm) brass rods of the same diameter placed in a copper pipe with an outside diameter of 8 mm (or 5 mm). This dimension determined the spatial resolution of the sensors. Their temporal resolution, found experimentally, was 2 μsec. The design of the sensors is described in greater detail in [10]. The forms of the pressure curves coincided for all three distances, but the amplitudes differed: the pressure 3.5 cm from the axis was lower than the pressure 6 and 8.5 cm from the axis by a factor of 1.3. The amplitudes were roughly equal at 6 and 8.5 cm. In absolute values, $p(3.5) \simeq 15$ MPa, $p(6) \simeq p(8.5) \simeq 20$ MPa. This difference can be attributed to manufacturing flaws in the piston and imperfect machining of the hammer face. However, as will be shown below, these flaws do not significantly affect the final result.

Figure 3 shows a pressure oscillogram (curve 1) obtained with the piezoelectric sensor located 3.5 cm from the axis. The second pressure maximum, separated from the first maximum by about 45 sec, is connected with the negative half-wave of the magnetic field. The parameters of the electrical circuit were such that the dischange of the battery through the coil was periodic in nature, with a moderate amount of decay. Curve 2 shows the oscillogram of the magnetic field in the gap between the end of the magnetic hammer and the piston. This oscillogram was obtained with a magnetic probe located 4 cm from the axis. In accordance

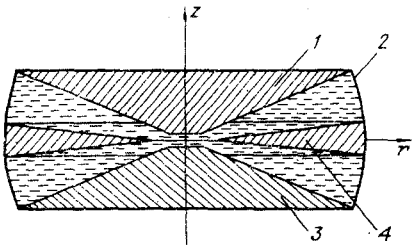

Fig. 5

Fig. 6

with Fig. 3, the duration of the compression wave at the half-amplitude is about 20 μsec, which corresponds to an effective pressure-pulse length of about 3 cm ($v_{so} \approx 1.5$ km/sec). The lag of the pressure maximum relative to the maximum of the magnetic field is due to the time required for passage of the wave from the piston to the end of the sensor. In the given case, the end of the sensor was located 2 cm from the piston.

Figure 4 shows the pressure oscillogram at the outlet of the concentrator 3 cm from the accumulation center (curve 3). The small sag in the pressure maximum is due to parasitic oscillations excited in the piezoelectric element by the rapid, strong shock – the so-called "ringing" of the sensor. The signal from the pressure sensor increased by a factor of about twenty over the case when the sensor was located near the piston. As is known, the piezoelectric modulus of a piezoceramic decreases with an increase in pressure – a phenomenon connected with reorientation of domains. However, it cannot be concluded on the basis of this that pressure was increased by a factor of more than twenty in the experiment (by a factor of thirty, for example). The fact is that the piezoelectric modulus decreases when the loading time is long. For short loading times (on the order of 1 μsec), the piezoelectric modulus of TsTS does not change up to 1.1 GPa [11]. The pressure build-up period in the experiment was 9 μsec. This is greater than the time in [11], but the measurements of pressure obtained with a quartz sensor gave the same gain as did measurements with the piezoceramic.

The nonuniformity of the pressure distribution in the pressure pulse near the piston should not significantly affect the pressure at the concentrator outlet, since the time of propagation of the pulse from the piston to the accumulation center (~320 μsec) is much longer than the time of sound propagation over the wavefront, and the pressure in the pulse has time to become equalized. Thus, even with a nonuniform pressure distribution in the initial pulse, pressure at the concentrator outlet will not differ significantly from the case of a uniform distribution if as the pressure in the pulse near the piston we take the average value of the nonuniform distribution over the area of the piston. Numerical calculations confirmed this. The theoretical curve 2 in Fig. 4 shows the time dependence of pressure at the concentrator outlet 3 cm from the accumulation center with a nonuniform pressure distribution in the pulse near the piston corresponding roughly to the experimentally measured distribution. It can be seen that the maximum pressure does not differ greatly from the measured pressure (line 3). The theoretical curve 1 reflects the time dependence of pressure in the pulse at the concentrator outlet for a uniform pressure distribution in the pulse near the piston. Here, we took a value of pressure equal to that obtained from averaging the nonuniform pressure distribution over the area of the piston – 17 MPa. It is evident from comparison of curves 1 and 2 that the difference in the maximum pressures is negligible.

It should be noted that the calculations were performed in a cylindrical geometry (Fig. 5) by means of a two-dimensional code, "RADAKS," which was developed previously [12]. Here, the cavity of the concentrator formed by two truncated cones 1 and 3 and the piston 2 was represented as a spherical layer of 50 cm radius. The ring 4, with conical surfaces, was represented by an inner cone 5 (see Fig. 2). It is clear that the theoretical and experimental schemes are identical for a uniform pressure distribution near the piston and are not identical for a nonuniform distribution; the nonuniformity is prescribed in the z direction in the theoretical scheme, while in the experimental scheme (see Fig. 2), pressure depends on the distance to the symmetry axis. However, this difference between the schemes is not crucial, since the mean pressures in both cases are about the same. Thus, the theoretical and experimental time dependences of pressure in the pressure pulse at the concentrator outlet coincide.

To increase the initial pressure without changing the parameters of the contour, we decreased the size of the gap between the piston and the end of the hammer. This increased the degree of nonuniformity of the pressure distribution over the piston, while the mean pressure

near the piston increased to 30 MPa. The insert 8 (see Fig. 2) was replaced by another insert with a smaller-diameter hole. This allowed us to stop the pressure pulse 1.5 cm from the accumulation center. The maximum pressure measured in this geometry was about 1 GPa, i.e. we obtained an increase by a factor of more than thirty in the intensity of a single pressure pulse. It should be noted that the leading edge of this pulse was seven times steeper than it initially was near the piston, while the leading edge was only twice as steep 3 cm from the accumulation center.

When a specimen is placed at the concentrator outlet, it will be subjected to an intensified pressure pulse. It is evident that if the specimen is made of a material with a compressibility lower than that of water, then the pressure in the specimen will be roughly equal to the pressure in the water directly adjacent to the specimen (it is assumed that the duration of the pulse is greater than the time of propagation of sound through the specimen). The case of a specimen having a high compressibility is more complicated (such as the case of a gas in a thin elastic shell). Here, the pressure in the specimen cannot be unambiguously determined, and appropriate numerical calculations must be performed in each specific case. In our experiments, we attempted to subject a stainless steel tube with an outside diameter of 4 mm and a wall thickness of 0.5 mm to a pressure of 1 GPa. The tube was asymmetrically deformed (Fig. 6), which was due to the development of Lavrentev–Ishlin instability with the mode k = 2. Thus, the scheme examined here also permits the compression of "soft" materials.

To obtain higher pressures, it is necessary to increase the pressure on the piston and to change the geometry of the concentrator in order to increase the degree of energy accumulation. Here, it should not be forgotten that a higher initial pressure in the pressure pulse leads to rapid steepening of the leading edge of the pulse, and the latter is changed into a shock wave. To avoid this, it is possible to either increase the length of the compression wave or to use a stiffer material than water as the transmitting medium (gallium, for example, which is liquid even at 30° C). Of course, the piston is no longer necessary when gallium is used. This simplifies the design of the system. Since the compressibility of the metal is much lower than the compressibility of water, an increase in the initial pressure by one order (to 300 MPa) with retention of the same length of compression wave leads to an increase of about one order in pressure near the accumulation center. The increase in pressure near the center is comparable to the increase in initial pressure because, under the given conditions, the wave will evolve in roughly the same manner. In other words, a system has now been fully developed for creating high pressures on the basis of the above-described scheme.

LITERATURE CITED

1. L. V. Alt'shuler, S. B. Kormer, et al., "Equations of state of aluminum, copper, and lead for the high-pressure region," Zh. Éksp. Teor. Fiz., 38, No. 3 (1960).
2. L. V. Al'tshuler, N. N. Kalitkin, et al., "Hugoniot curves at ultra-high pressures," Zh. Éksp. Teor. Fiz., 72, No. 1 (1977).
3. V. E. Fortov, "Dynamic methods in plasma physics," Usp. Fiz. Nauk, 138, No. 3 (1982).
4. E. N. Avrorin, B. K. Vodolaga, et al., "Shock compressibility of lead, quartzite, aluminum, and water at a pressure of about 100 Mbar," Pis'ma Zh. Éksp. Teor. Fiz., 31, No. 12 (1980).
5. R. S. Hawke, D. E. Duere, et al., "Method of isentropically compressing materials to several megabars," J. Appl. Phys., 43, No. 6 (1972).
6. A. I. Pavlovskii, N. P. Kolkol'chikov, et al., "Isentropic compression of quartz by pressure from an ultrahigh-strength magnetic field," Pis'ma Zh. Éksp. Teor. Fiz., 27, No. 5 (1977).
7. S. G. Alikhanov, V. P. Bakhtin, et al., "High-pressure generation by means of pulsed magnetic fields," in: High-Pressure Science and Technology: Proc. 6th AIRAPT Conf., Plenum Press, New York, London (1979), Vol. 2.
8. V. V. Prut, V. A. Khrabrov, et al., "Metallic z-pinch method: isentropic compression of hydrogen," Pis'ma Zh. Eskp. Teor. Fiz., 29, No. 1 (1979).
9. Ya. B. Zel'dovich and Yu. P. Raizer, Physics of Shock Waves and High-Temperature Gasdynamic Phenomena, Fizmatgiz, Moscow (1963).
10. S. G. Alikhanov and V. P. Bakhtin, "A piezoelectric pressure bar gauge with mechanical sandwiching of the piezoelement," J. Phys. E., 16, 615 (1983).
11. C. E. Reynolds and G. E. Seay, "Two-wave shock structure in ferroelectric ceramics barium titanate and lead zirconate–titanate (PZT)," J. Appl. Phys., 33, No. 7 (1962).
12. S. G. Alikhanov and V. P. Bakhtin, "Use of m = 0 instability for three-dimensional compression of a plasma," Dokl. Akad. Nauk SSSR, 263, No. 2 (1982).